RSC Advances

RSC Publishing

PAPER

View Article Online
View Journal | View Issue

Cite this: *RSC Advances*, 2013, **3**, 18367

Green synthesis of Au, Pd and Au@Pd core–shell nanoparticles *via* a tryptophan induced supramolecular interface†

Sarvesh Kumar Srivastava,[a] Takashi Hasegawa,[a] Ryosuke Yamada,[b] Chiaki Ogino,[a] Minoru Mizuhata[a] and Akihiko Kondo*[a]

Received 3rd July 2013,
Accepted 22nd July 2013

DOI: 10.1039/c3ra43389g

www.rsc.org/advances

A facile, eco-friendly, room-temperature method for rapid one-pot synthesis of Au@Pd bimetallic nanoparticles exhibiting a core–shell morphology (~60 nm) has been developed based on the successive reduction of Au(III) and Pd(II) precursors with tryptophan (Trp) in an aqueous environment. The unique supramolecular chemistry arising due to the hydrogen bonded indole group layer over the Au core seemed critical in the formation Pd shell. The core–shell morphology and surface analysis of the resulting Au@Pd nanoparticles were confirmed by aberration corrected scanning transmission electron microscopy followed by X-ray photoelectron spectroscopy. The formation of the core (Au) and shell (Pd) was also confirmed by Energy Dispersive X-Ray elemental scanning analysis. The resulting Au, Pd and Au@Pd nanoparticles were also analysed by UV-Vis spectroscopy, X-ray diffraction and Dynamic Light Scattering. Our results suggest a simple coordination mechanism where the pre-stabilized poly-Trp Au core serves as a template to facilitate the subsequent reduction of Pd(II) *via* active carboxyl groups. This study effectively demonstrates for the first time that core–shell nanoparticle synthesis (reduction and stabilization) can be effectively achieved by simple amino acids like Trp in an aqueous reaction mixture.

Introduction

Bimetallic nanoparticles have gained importance because of their composition dependent optical, catalytic and magnetic properties which are different compared to their monometallic counterparts.[1] Au@Pd bimetallic nanoparticles with core–shell morphology in particular have proved to be an excellent catalyst for a variety of reactions including oxidation reactions which are of importance in the field of fuel cells,[2] semiconductors,[3] drug delivery[4] and so on. A number of strategic routes have been proposed for the synthesis of core–shell structures including Toshima's sacrificial hydrogen method,[5] surface-specific reductants,[6] galvanic displacements,[7] controlled simultaneous reduction[8] and exploitation of core/shell preferences through annealing.[9] However, most of these methods require stringent process control, expensive instruments and usage of several toxic solvents *etc*. Therefore, there is an urgent need to produce these valuable bimetallic structures in a more sustainable and eco-friendly manner.

Biogenic synthesis of nanomaterials has recently gained a lot of importance by utilizing naturally occurring compounds as the basis for new material synthesis. We have demonstrated a range of biogenic materials in the form of monometallic nanoparticle synthesis[10] for the preparation of heterogeneous catalysts *via* bacteria[11] covering an array of nanoparticles including Au, Ag, Pd, Fe, Rh, Ni, Ru, Pt, Co, and Li. These bio-inspired materials have advanced chemical properties with inherent potential to support a variety of novel technologies. Recently, Huang *et al.*[12] reported Au@Pd core–shell nanoparticles *via* plant tannin as reductant and stabilizer. Although, biogenic nanoparticle synthesis is still in its infancy, these studies, among others, clearly demonstrated that multiple complex reactions and subsequent stabilization, especially in the case of bimetallic nanoparticles,[13–15] can be achieved by biological entities.

However, it should be noted that while alloyed nanoparticles are relatively easy to produce, synthesis of discreet stable core–shell structures *via* biogenic means still remains a challenge. This can be understood because one of the key characteristics of biogenic synthesis is the 'cumulative effect' of the active reaction mixture generally consisting of large complex molecules or compounds which may be difficult to isolate or purify. This remains a major drawback in most biogenic processes limiting their use in large scale production. Therefore, there is a need to target smaller active chemical

[a]*Department of Chemical Science and Engineering, Graduate School of Engineering, Kobe University, 1-1 Rokkodai-cho, Nada, Kobe, 657-8501, Japan. E-mail: akondo@kobe-u.ac.jp; Fax: +81-78-803-6196; Tel: +81-78-803-6196.*
[b]*Organization of Advanced Science and Technology, Kobe University, 1-1 Rokkodai-cho, Nada, Kobe, 657-8501, Japan. E-mail: ryo-_-7@dolphin.kobe-u.ac.jp*

† Electronic supplementary information (ESI) available: TEM, STEM and catalytic degradation data of Au, Pd and Au@Pd nanoparticles. See DOI: 10.1039/c3ra43389g

groups present in the 'biogenic broth' in order to assist biogenic studies to evolve towards biomimetic technologies.

Amino compounds including amino acids show promise as biosynthesis agents which have been tested as effective reducing agents for the preparation of monometallic nanoparticles.[16,17] These amino acids in aqueous environments exhibit their characteristic zwitterion structure which has the potential to impart additional supramolecular functionality and stability to bimetallic nanoparticles. This amino group mediated supramolecular functionality is important in the synthesis and stabilization of core–shell structures as demonstrated by Serpell *et al.*[18] by imparting anion distribution *via* imidazole–amide linkages. Tryptophan is one such interesting amino acid which has the unique chemical properties of reducing and stabilizing metallic nanoparticles. Several studies showed that tryptophan plays an important role in the reduction of monometallic nanoparticles (Au) *via* the oxidation of the amino acid and forms poly-Trp which caps and stabilizes the resulting nanoparticles.[19,20]

In this study, we demonstrate for the first time, the biosynthesis of Au@Pd bimetallic nanoparticles *via* tryptophan in aqueous reaction mixture at room temperature. Gold seeds were produced by incorporating tryptophan in the reaction mixture followed by the successive reduction of Pd over the gold nanoparticle surface. To confirm the nature of the nanoparticles and responsible chemical groups, various characterization techniques including UV-Vis spectroscopy, transmission electron microscopy (TEM), aberration-corrected high angle annular dark field scanning transmission electron microscopy (AC-HAADF-STEM), energy dispersive spectrometry (STEM-EDS), zeta-potential analysis, X-ray diffraction (XRD) and X-ray photoelectron spectroscopy (XPS) were employed. These analyses suggested the formation of Au@Pd core–shell type bimetallic nanoparticles in the aqueous reaction mixture due to anion coordination functionality imparted by the poly-Trp layer around the seed Au nanoparticles. The use of Trp as a reducing and stabilizing agent to obtain bimetallic nanoparticles with core–shell morphology has potential to be a facile, cost-effective, one-pot green synthesis of multimetallic nanoparticles in future.

Experimental section

(a) Synthesis of Au, Pd and Au@Pd nanoparticles

Chloroauric acid ($HAuCl_4$) and palladium chloride ($PdCl_2$) were obtained from Aldrich (Tokyo, Japan) and were used directly without pre-treatment. L-Tryptophan was obtained from Nacalai tesque (Kyoto, Japan).

Ultrapure water (resistivity $\sim$18.2 MΩ cm) was used as a solvent throughout the experiments. A well-mixed gold cation stock solution at 0.5 mM (10 mL) and palladium cation stock solution (0.5 mM, 10 mL) were prepared. To prepare the Pd(II) ionic solution, pre-weighed $PdCl_2$ was introduced into 5 mL of 5 mM HCl followed by volume make-up by addition of ultrapure water. A Trp aqueous stock solution was prepared at a concentration of 0.5 mM (20 mL). Cation solutions consisting of Au : Pd were used in the volumetric ratio of 1 : 1. A gold nanoparticle solution was prepared by the spontaneous reduction of 10 mL gold cation solution in the presence of 2 mL of Trp solution with vigorous stirring for 2 h followed by intermittent sonication for 30 s at every 15 min. Au NPs prepared at this stage served as a seed (core) for the deposition of Pd (shell) along the surface of the Au NPs. It should be noted that the size of the core–shell structures can be controlled by controlling the size of the Au NPs at the seeding stage. For Au@Pd bimetallic nanoparticles, a palladium precursor solution (5 mL) was introduced to the gold NP seed solution (5 mL) along with 1 mL of Trp solution. The resulting mixture was stirred for 2 h followed by intermittent sonication for 10 s at every 30 min. The Pd NP solution was prepared in the same way as mentioned above for the Au NP seed synthesis. Therefore, three distinct types of nanoparticles were synthesized namely Au NPs, Pd NPs and Au@Pd NPs.

(b) Characterization of Au, Pd and Au@Pd nanoparticles

UV-visible spectra were obtained using a JASCO V670 UV-vis Spectrophotometer. Nanoparticle formation was monitored from 400–800 nm at a 2000 nm min^{-1} scan rate. This was done as the focus of this study was in the visible region (LSPR) which provided vital details about the Au@Pd bimetallic nanoparticle formation. Morphology and grain size analysis of these nanoparticles (Au, Pd, Au@Pd NPs) was carried out using a JEOL JEM-2010 transmission electron microscope (TEM) operating at an acceleration voltage of 200 kV. One micro-litre was taken from the reaction mixtures and placed on carbon coated copper grids and dried at room temperature. The images were analysed using ImageJ 1.43 M software. Individual Au@Pd nanoparticles were further analysed by aberration-corrected STEM-HAADF microscopy (JEOL 2100F, 200 kV, $\sim$0.1 nm point resolution) to observe the precise structure of the resulting core–shell nanoparticles. Observed nanoparticles were also analysed by JED-2300T STEM-EDS to obtain the composition architecture.

X-ray diffraction (XRD) patterns were obtained using a Rigaku RINT-TTR diffractometer equipped with a parallel beam collimation and a vertical θ–θ goniometer. Samples were placed directly onto a sample holder. The X-ray diffractometer was operated at 50 kV and 300 mA to generate the Cu-Kα radiation. The scan rate was set to 5° min^{-1}.

Zeta-potential measurements were performed using a Malvern Zetasizer Nano ZS model ZEN3600 (Worcestershire, UK) equipped with a standard 633 nm laser.

Surface analysis for the Au@Pd bimetallic NPs was also carried out by X-ray photoelectron spectroscopy (XPS) obtained from a JEOL JPS9010 MC photoelectron spectrometer operating at 10 kV and 30 mA to generate (Al)Kα radiation. The results obtained were analysed by SpecSurf ver. 1.7.3.9 software.

Results and discussion

Of the two general approaches for synthesizing bimetallic nanoparticles, a successive reduction approach normally gives better control over the shape and atomic ratio as compared to

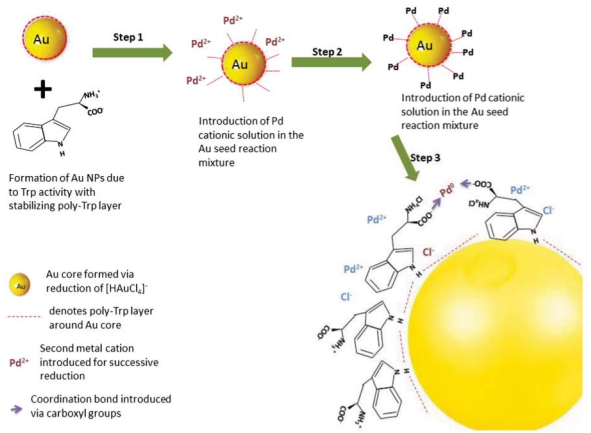

Fig. 1 Schematic representation of anion coordination synthetic strategy for Au@Pd nanoparticles.

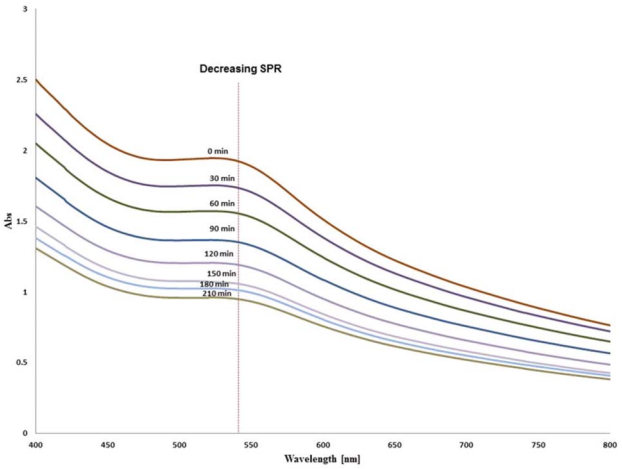

Fig. 3 Visible spectra showing formation of Pd layer over the synthesized Au core. Each line denotes an interval of 30 min.

a simultaneous approach especially with respect to the core–shell structure. For the same reason, we utilized a successive reduction approach to yield Au@Pd bimetallic NPs with core–shell structures. The synthesis strategy used in this work has three steps as hypothesized in Fig. 1.

Firstly, Au core nanoparticles were formed and stabilized *via* a poly-Trp layer due to indole group H-bonded supramolecular functionality.[21,22] Next, the shell metal (Pd II) was introduced into the aqueous reaction mixture in its cationic state which associated with the core ligands (*via* Trp). This results in the sequestering of Pd(II) onto the surface of the Au core *via* the active carboxyl groups. Finally, the surface bound Pd(II) was reduced over the Au core, yielding the core–shell structures.

Fig. 2 shows the UV-vis absorbance spectra of the Trp synthesized Au@Pd nanoparticles and reaction mixtures of monometallic Au and Pd nanoparticles. The color change between the three reaction mixtures was visually distinguishable after the completion of the reaction. Gold nanoparticles can be seen with a distinct pink color, while the Au@Pd NP solution turned black-brown followed by the orange-brown color of the Pd NP solution (inset Fig. 2).

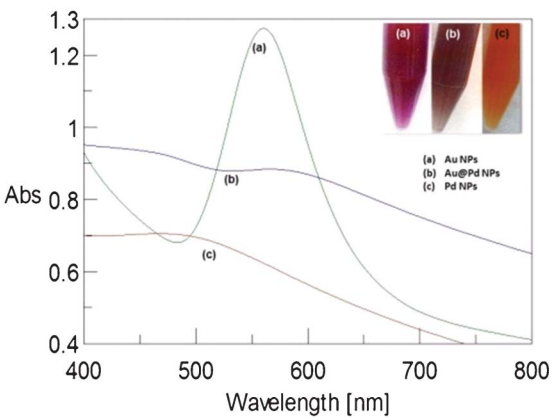

Fig. 2 Visible spectra of Au, Pd and Au@Pd nanoparticles. Inset image depicting observed color in each of the above mentioned reaction mixtures.

These results also suggest that the bimetallic nanoparticle (Au@Pd) mixtures present in the reaction solution are not phase separated when compared with monometallic NPs. Au NPs showed a characteristic localized surface plasmon resonance (LSPR) peak centered at 550 nm. The LSPR peak was drastically reduced in the case of the Au@Pd bimetallic NPs and completely absent in the case of the Pd NP reaction mixture after the completion of reaction. This spectral behaviour reasonably indicates the core–shell structure. In such closely associated structures (like core–shell), the surface electron density in the Au core increases at the expense of electrons from the outer Pd shell. This happens because Pd has a higher electron chemical potential (5.32 eV *vs.* 5.00 eV). Thus, a thicker Pd shell coating on the Au core results in the gradual damping of the plasmon of the Au core.[23]

To further confirm the interaction between the Au NP surface and subsequent Pd deposition, UV-vis spectroscopy was carried out (400–800 nm) to observe the coating of Pd over the Au core as a function of time as shown in Fig. 3.

Each successive spectrum was taken at a 30 min interval up to three hours. This also confirmed that the reaction (deposition of Pd over Au) nearly reached completion after 3 h. The gradual decrease in LSPR can be easily observed at around 550 nm as the reaction proceeds to completion. This also suggests that the Pd shell thickness can be controlled by varying reaction time while keeping the other parameters constant. Overall, UV-vis analysis strongly suggested a chemical interaction between the Au nanoseed surface and the subsequent coating deposition of palladium. To confirm and characterize the formation of Au@Pd bimetallic nanoparticles with core–shell morphology in the solution, we carried out TEM followed by high resolution STEM and EDS. TEM imaging (Fig. 4) confirmed truncated octahedral type Au NPs of around 50 nm in size in the reaction mixture as shown in Fig. 4a.

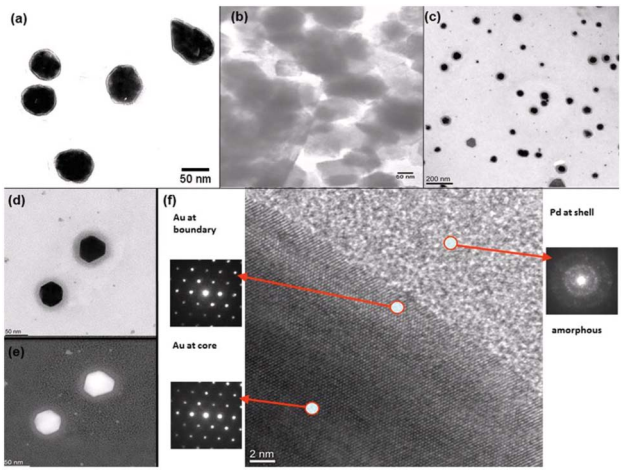

Fig. 4 TEM images of (a) Au NPs, (b) Pd NPs, (c) Au@Pd NP population, (d) individual Au@Pd NPs (as shown in 4c), (e) AC-STEM-HAADF imaging of individual Au@Pd NPs, (f) STEM imaging of individual Au@Pd NP boundary layer.

The observed Au NPs were highly dispersed over the sample grid as Trp has already been proved to be an efficient reducing and capping agent for Au NPs. However, unlike the Au NPs, the Pd NPs lacked shape control and showed a greater degree of aggregation as shown in Fig. 4b. TEM analysis of the Au@Pd bimetallic nanoparticle population showed well dispersed Au@Pd bimetallic nanoparticles. Fig. 4e shows individual Au@Pd NPs (as highlighted in Fig. 4c) where the dense Au core can be clearly seen surrounded by the Pd layer. We observed Au@Pd NPs in the range of ~60 nm where the Au core size was about ~50 nm and Pd shell thickness was in the range of 5–10 nm.

Aberration-corrected high-angle annular dark-field scanning TEM (AC-HAADF-STEM) was used to confirm the core–shell morphology of the observed Au@Pd NPs. HAADF-STEM imaging (Fig. 4e) displayed a brighter gold core due to its heavier atomic weight while the palladium shell appeared comparatively less bright due to its low atomic weight. A highly discreet Au@Pd boundary layer was also observed (Fig. 4f) where the Au core in the center showed a characteristic Au (111) diffraction pattern. Also, in the absence of any distinct diffraction pattern, the Pd shell was rather amorphous in nature. Thus, the Au@Pd NPs observed in this study largely comprise of a crystalline Au core with a largely amorphous Pd shell. This was further confirmed by subsequent XRD analysis of Au, Pd and Au@Pd NPs as shown in Fig. 5.

As observed from XRD, the truncated octahedron Au NP seeds (Fig. 5a) showed a very strong Bragg diffraction at (111) at 38.05° followed by a very weak diffraction at 44.57° which can be assigned to the (200) crystal plane. In the case of the Au@Pd NPs (Fig. 5b), a distinct peak was observed at 68.19° suggesting a Au (220) crystal re-arrangement normally observed in core–shell structures. Finally, no credible peaks can be assigned to Pd for the Pd NPs (Fig. 5c) and Au@Pd NPs confirming that the majority of reduced palladium was

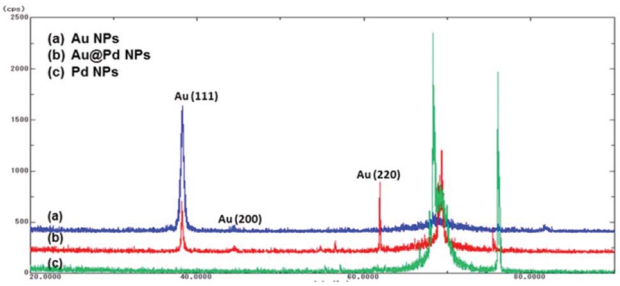

Fig. 5 XRD patterns of (a) Au NPs, (b) Au@Pd NPs, (c) Pd NPs.

amorphous in nature. This can be understood as the observed reductive reaction under the supramolecular effect of Trp is rather quick when Pd(II) ions are reduced to Pd atoms. Hence, the resulting Pd atoms are produced rapidly at room temperature where Pd atoms stick onto particles without relaxation/surface tension to balance sites thereby producing a disordered structure *i.e.* the amorphous state of palladium.[24]

STEM-EDS elemental mapping was used to verify the element distribution over the observed Au@Pd NPs (Fig. 6).

Colored elemental mapping images showed that Au atoms (red, Fig. 6b) and Pd atoms (green, Fig. 6a) were discreetly distributed with dense a Au core at the centre and Pd at the boundary giving rise to a characteristic core–shell structure (Fig. 6c). EDS elemental line scanning (Fig. 6d) on the single particles confirmed that the Au@Pd NPs (~60 nm) were composed of a distinct Au rich centre and Pd rich boundary responsible for typical core–shell (not alloyed) morphology. This analysis reveals the presence of both Au and Pd in the same nanoparticle. As the concentration of Au is higher in the NP under observation, the signal of Au is more intense than that of the Pd. However, careful observation also reveals that the signal of Pd is slightly broader than that of the Au. This indicates the existence of Pd as the shell and Au as the core. It must be noted that the interaction profile between Au and Pd

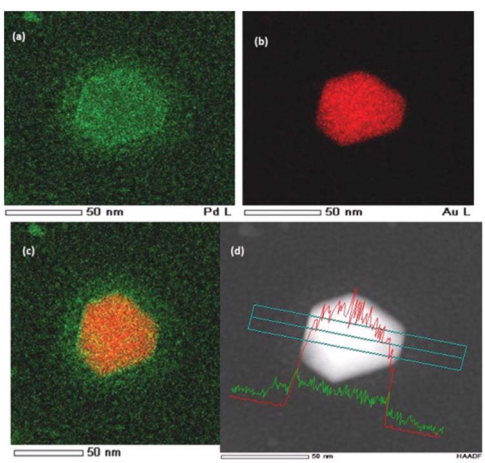

Fig. 6 STEM-EDX elemental mapping of (a) Pd, (b) Au, (c) Au@Pd NP (overlay), (d) line profile of resulting Au@Pd NP.

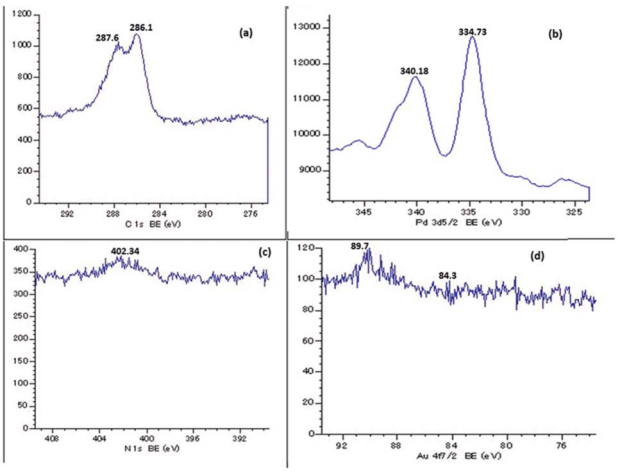

Fig. 7 XPS spectra of Au@Pd NPs exhibiting following regions as (a) C 1s (b) Pd 3d (c) N 1s and (d) Au 4f.

largely depends on the particle shape and order of the two metallic species. Similar HAADF-STEM results for Au@Pd NPs were also reported by Han *et al.*[25]

These Au@Pd nanoparticles exhibiting core–shell morphology were further subjected to XPS analysis (Fig. 7) to confirm the metallic nature of the Au and Pd along with the responsible chemical groups present in the reaction mixture. The metallic shell of Pd was confirmed (Fig. 7b) by characteristic Pd 3d 5/2 and Pd 3d 3/2 peaks at 340.18 eV and 334.73 eV respectively. The Au core was denoted at 89.7 eV and 84.3 eV as observed in Fig. 7d. Since Trp was the only active chemical agent used in this reaction, an interesting observation was made when C 1s and N 1s (Fig. 7a, c) XPS spectra of Au@Pd were observed (amino and carboxyl ends).

The doublet in the C 1s spectra showed the presence of a carboxyl group at 286.05 eV along with the probable presence of an amine carboxyl (NH–C=O) peak at 287.6 eV. Further, the N 1s spectra showed the presence of NH_4Cl (402.3 eV) in the reaction mixture.

Based on the reduction potential of Au(III) and Pd(II) ($AuCl^{4-}$/Au, +1.002 *vs.* SHE (standard hydrogen electrode) and Pd^{2+} ($PdCl^{2-}$/Pd, +0.915 V *vs.* SHE), we can easily expect that the Au(III) will be preferentially reduced over the Pd(II) under our experimental reaction conditions.[26] In another study by Lee *et al.*[27] the synthesis of Au@Pd core–shell nanooctahedrons by utilizing CTAC as both a reducing and stabilizing agent was reported. Similarly, in our reaction mixture, Trp plays a key role in the reduction and subsequent stabilization of the core–shell structure. The presence of the indole functional group together with the amine and carboxyl groups is the important structural characteristic of the aromatic amino acid residue tryptophan. Studies have shown that the salt-bridge structure involving the COOH group appears to be energetically more favourable than the two comparably interacting indole and NH_2 groups.[28] This leaves the indole group free to stabilize the resulting Au NP *via* indole polymerization (poly-Trp) obtained by the hydrogen linking between the N-group of the interacting indole groups and followed by the deposition of palladium over the Au NP surface in the presence of NH_3^+ and the COO^- zwitterion state.

Zeta-potential analysis of all three NP reaction mixtures was carried out to understand the relative stability of the resulting nanoparticles in aqueous solution. Au NPs synthesized *via* Trp showed a high stability in the aqueous reaction mixture with average zeta-potential as +18.8 eV clearly due to the presence of the indole polymerized surface granting extra stability to the Au NPs along with the exposed amino groups (NH_3^+). Therefore, in order to achieve Pd deposition over the Au surface, chemical interactions involving free NH_3^+ amino groups with PdCl over the indole polymerized surface should result in a decreased zeta-potential (as observed by XPS by the formation of NH_4Cl). The resulting Au@Pd NPs demonstrated a mean zeta potential of −2.26 eV suggesting that the resulting bimetallic nanoparticles with core–shell morphology are somewhat stable in the aqueous reaction mixture. This decrease in positive charge can be attributed to the quenching of the free amino groups present along the indole group stabilized Au NP surface. Pd NPs showed a mean zeta-potential of −0.07 eV suggesting greater particle aggregation in the reaction mixture as observed earlier by TEM.

We believe that the temporal separation of the formation of the Au octahedron from the formation of the Pd layer owing to the presence of capping properties of Trp and associated coordination supramolecular chemistry is the key to the formation of the core–shell structure. The new structural arrangement in the Au@Pd NPs confirmed the core–shell nature of the resulting nanoparticles. This novel green process promises Trp as a potential agent for the synthesis and stabilization of bimetallic nanoparticles with core–shell morphology (like Au@Pd NPs). Finally, catalytic efficiency of the synthesized Au, Pd and Au@Pd NPs was tested by the degradation of 4-nitrophenol (see supplementary information†).

Conclusion

In summary, we presented a simple one-pot green synthesis of Au NPs, Pd NPs and Au@Pd bimetallic NPs with core–shell structures. Since the focus of this study was towards the Au@Pd bimetallic NPs, we observed a Au octahedron core (~50 nm) with a Pd layer (~5 nm) forming the shell. This Pd layer deposition was found to be time dependent keeping other reaction parameters constant. The resulting NPs were characterized by TEM, XRD and zeta-potential analysis. Further, the Au@Pd NPs were analysed by AC-HAADF-STEM, STEM-EDS and XPS to confirm and analyse the resulting core–shell morphology. Although a lot of research has been put into the study of bimetallic nanoparticles (with emphasis on the core–shell structure), our study demonstrates for the first time, the synthesis of stable Au@Pd bimetallic nanoparticles (core–shell type) by the successive reduction approach in the presence of an amino acid (Trp) at room temperature. The

resulting nanoparticles will find numerous applications in the study of physiochemical properties of heterostructured nanomaterials and several other catalytic applications. Further, tryptophan will not induce any biological toxicity as compared to other chemical counterparts and nanoparticles synthesized by this technique may find several important uses in biological systems and diagnostics due to their inherent UV fluorescence. Interdisciplinary research will aid in the better understanding of the underlying mechanisms and process improvement.

Acknowledgements

This work was partly supported by the Special Coordination Fund for Promoting Science and Technology, Creation of Innovative Centers for Advanced Interdisciplinary Research Areas (Innovative Bioproduction Kobe) from the Ministry of Education, Culture, Sports and Technology (MEXT) and partly by the MEXT Scholarship research fund.

Notes and references

1 N. Toshima and T. Yonezawa, *New J. Chem.*, 1998, **22**, 1179.
2 W. Zhou and J. Y. Lee, *Electrochem. Commun.*, 2007, **9**, 1725.
3 K. J. Major, C. De and S. O. Obare, *Plasmonics*, 2009, **4**, 61.
4 K. S. Soppimath, D. C. W. Tan and Y. Y. Yang, *Adv. Mater.*, 2005, **17**, 318.
5 N. Toshima, Y. Shiraishi, A. Shiotsuki, D. Ikenaga and Y. Wang, *Eur. Phys. J. D*, 2001, **16**, 209.
6 K. R. Brown and M. J. Natan, *Langmuir*, 1998, **14**, 726.
7 W. R. Lee, M. G. Kim, J. R. Choi, J. I. Park, S. J. Ko, S. J. Oh and J. Cheon, *J. Am. Chem. Soc.*, 2005, **127**, 16090.
8 K. Mallik, M. Mandal, N. Pradhan and T. Pal, *Nano Lett.*, 2001, **1**, 319.
9 K. J. Mayrhofer, V. Juhart, K. Hartl, M. Hanzlik and M. Arenz, *Angew. Chem., Int. Ed.*, 2009, **48**, 3529.
10 S. K. Srivastava and M. Constanti, *J. Nanopart. Res.*, 2012, **14**, 831.
11 S. K. Srivastava, R. Yamada, C. Ogino and A. Kondo, *Nanoscale Res. Lett.*, 2013, **8**, 70.
12 X. Huang, H. Wu, S. Pu, W. Zhang, X. Liao and B. Shi, *Green Chem.*, 2011, **13**, 950.
13 G. Zhan, J. Huang, M. Du, I. A. Rauf, Y. Ma and Q. Li, *Mater. Lett.*, 2011, **65**, 2989.
14 P. S. Schabes-Retchkiman, G. Canizal, R. Herrera-Becerra, C. Zorrilla, H. B. Liu and J. A. Ascencio, *Opt. Mater.*, 2006, **29**, 95.
15 S. Senapati, A. Ahmad, M. I. Khan, M. Sastry and R. Kumar, *Small*, 2005, **1**, 517.
16 X. Liu, J. Zhang, X. Guo, S. Wu and S. Wang, *Nanoscale*, 2010, **2**, 1178.
17 R. R. Naik, S. J. Stringer, G. Agarwal, S. E. Jones and M. O. Stone, *Nat. Mater.*, 2002, **1**, 169.
18 C. J. Serpell, J. Cookson, D. Ozkaya and P. D. Beer, *Nat. Chem.*, 2011, **3**, 478.
19 P. R. Selvakannan, S. Mandal, S. Phadtare, A. Gole, R. Pasricha and S. D. Adyanthaya, *J. Colloid Interface Sci.*, 2004, **269**, 97–102.
20 M. Iosin, P. Baldeck and S. Astilean, *J. Nanopart. Res.*, 2010, **12**, 2843.
21 J. D. Newman and G. J. Blanchard, *Langmuir*, 2006, **22**, 5882.
22 S. Si and T. K. Mandal, *Chem.–Eur. J.*, 2007, **13**, 3160–3168.
23 J. W. Hu, Y. Zhang, J. F. Li, Z. Liu, B. Ren, S. G. Sun, Z. Q. Tian and T. Lian, *Chem. Phys. Lett.*, 2005, **408**, 354.
24 W. Lu, B. Wang, K. Wang, X. Wang and J. G. Hou, *Langmuir*, 2003, **19**, 5887.
25 J. W. Hong, D. Kim, Y. W. Lee, M. Kim, S. W. Kang and S. W. Han, *Angew. Chem. Int. Ed.*, 2011, **50**, 8876.
26 K. Y. Lee, M. Kim, Y. W. Lee, J. J. Lee and S. W. Han, *Chem. Phys. Lett.*, 2007, **440**, 249.
27 Y. W. Lee, M. Kim, Z. H. Kim and S. W. Han, *J. Am. Chem. Soc.*, 2009, **131**, 17036.
28 P. Joshi, V. Shewale, R. Pandey, V. Shanker, S. Hussain and S. P. Karna, *J. Phys. Chem. C*, 2011, **115**, 22818.

